Published in final edited form as:
Invest Ophthalmol Vis Sci. 2007 October ; 48(10): 4616–4625. doi:10.1167/iovs.07-0233.

Altered Chemokine Profile Associated with Exacerbated Autoimmune Pathology under Conditions of Genetic Interferon-γ Deficiency

Shao Bo Su, **Rafael S. Grajewski**, **Dror Luger**, **Rajeev K. Agarwal**, **Phyllis B. Silver**, **Jun Tang**, **Jingsheng Tuo**, **Chi-Chao Chan**, and **Rachel R. Caspi**
From the Laboratory of Immunology, National Eye Institute, National Institutes of Health, Bethesda, Maryland

Abstract

Purpose—A prior study showed that mice deficient in IFN-γ (GKO) are more susceptible to experimental autoimmune uveitis (EAU) than are wild-type (WT) mice. Histopathology of uveitic eyes revealed that the ocular infiltrate in GKO mice was dominated by neutrophils and eosinophils rather than by mononuclear cells, as in WT mice. The present study was conducted to explore the differential expression of chemokine(s) likely to account for the distinct inflammatory cell composition in uveitic eyes of WT and GKO mice.

Methods—Mice were immunized to induce EAU. Lymph nodes draining the site of the immunization and the eyes were collected at different time points for chemokine analysis. Microarray, real-time PCR and protein analyses were performed to examine the expression of chemokines in WT and GKO mice.

Results—Many chemokines were differentially upregulated in GKO versus WT mice. Expression of the Th1-associated chemokines CXCL10, CXCL9, CCL5, and CXCL11 was elevated in WT mice, whereas the Th2-associated chemokines CCL11, CCL17, and CCL1 and the Th17-associated chemokines CCL22 and CXCL2 were elevated in the GKO mice. Depletion of granulocytes abrogated EAU in both WT and GKO mice.

Conclusions—These results suggest that Th1-associated chemokines play a critical role in the attraction of mononuclear cells to the eyes in the presence of IFN-γ, while in the absence of this cytokine, Th2- and Th17-related chemokines may be the key elements for influx of granulocytes.

Experimental autoimmune uveoretinitis (EAU) is an organ-specific, $CD4^+$ T-cell–mediated disease, that can be induced in genetically susceptible strains of mice after immunization with retinal proteins, such as interphotoreceptor retinoid– binding protein (IRBP) or S-antigen (arrestin), or by the adoptive transfer of T-cells specific for these antigens.[1,2] EAU is characterized by granulomatous inflammation in the neural retina, vasculitis, destruction of photoreceptor cells, and blindness.[3,4] The pathology seen in EAU strikingly resembles human uveitic diseases of putative autoimmune etiology, such as ocular sarcoidosis and Behçet's disease[3–5] and serves as a model for these diseases, as well as a model for organ-specific autoimmunity mediated by T-cells. Effector T-lymphocytes can be divided into several subsets including Th1, Th2, and Th17, based on their patterns of cytokine production.[6–13] Th-1 type

Corresponding author: Rachel R. Caspi, Laboratory of Immunology, National Eye Institute, National Institutes of Health, 10 Center Drive, 10/10N222, Bethesda, MD 20892-1857; rcaspi@helix.nih.gov.

Disclosure: S.B. Su, None; R.S. Grajewski, None; D. Luger, None; R.K. Agarwal, None; P.B. Silver, None; J. Tang, None; J. Tuo, None; C.-C. Chan, None; R.R. Caspi, None

cells secrete interferon (IFN)- γ and IL-2, and are responsible for directed cell-mediated immune responses such as delayed-type hypersensitivity (DTH). Th2 cells secrete IL-4, Il-5, and IL-13 and are involved in humoral immunity and allergic responses. Th17 cells secrete IL-17, TNF-α, and IL-6, and have been implicated in inflammatory responses. Previous data from our laboratory showed that depletion of systemic IFN-γ by anti IFN-γ antibodies exacerbates disease in the mouse EAU model, and some strains normally resistant to EAU-induction develop disease after treatment with anti-IFN-γ antibodies.[14] Furthermore, IFN-γ-deficient (GKO) mice are more susceptible to EAU and to EAE compared with their wild-type (WT) control littermates. [15,16] Of note, GKO mice develop a deviant effector response that differs from that of wild-type mice, in that it contains a prominent component of granulocytes in the inflammatory infiltrate, resembling the responses in Th2-mediated diseases.[15–17]

Entry of immune cells into and their retention and activation within tissues are crucial features of host immune response against pathogens and of autoimmune pathogenesis. The migration of immune cells to target organs depends on the gradient of chemokines in the inflammatory sites. Chemokines are a group of small (8 –10-kDa), secreted polypeptides and can be divided into families based on their structure—in particular, the motif of the first two of four cysteine residues in their amino acid structure. The largest family, CCL, has cysteine residues adjacent to each other, whereas the CXCL family has an intervening amino acid between the cysteine residues. Two smaller families XCL (containing only two cysteine residues) and CX3CL (with three intervening amino acids) complete the chemokine group.[18,19] The migration of leukocytes induced by chemokines is based on the expression of cognate chemokine receptors on leukocytes. Each subset of immune cells expresses various levels of chemokine receptors. Th1 T cells predominantly express CXCR3 and CCR5. Therefore, the main cognate ligands for these receptors, CXCL9, CXCL10, CXCL11, and CCL5, are known as Th1-associated chemokines.[20,21] Th2 selectively express CCR3, CCR4, and CCR8. The main cognate ligands for these receptors, CCR8, CCL11, CCL17, and CCL1, are known as Th2-associated chemokines.[21,22] The Th2 chemokines also attract granulocytes. The recently described Th17 effectors are associated with CCL6, CXCL2 (the murine IL-8 equivalent) CCL7, CCL20, and CCL22.[23,24]

Chemokines are critical mediators in the pathogenesis of many diseases. For example, CCL3, CCL2, CCL5, CXCL9, and CXCL10 are upregulated in the eyes at the onset of EAU.[25–27] Fife et al.[28] reported that CXCL10 is a crucial chemokine in the recruitment and accumulation of inflammatory mononuclear cells during the pathogenesis of EAE. Our previous data showed that blockade of chemokine signaling by pertussis toxin during the effector stage of EAU abrogates disease development. [29] In the present study, we examined the expression of chemokines in uveitic IFN-γ-deficient and wild-type C57BL6 mice. We found that the Th1-associated chemokines, CXCL10, CXCL9, CCL5, and CXCL11 were highly expressed in wild-type mice and were associated with a mononuclear infiltration into the eyes. In contrast, the Th2-associated chemokines CCL11, CCL17, and CCL1 and the Th17-associated chemokines CCL22 and CXCL2 were upregulated in GKO mice and were associated with a predominantly granulocytic infiltrate. These cytokine profiles may explain the differential recruitment of leukocyte subpopulation into uveitic eyes in the absence versus presence of an IFN-γ response. Importantly, as indicated by depletion studies, granulocytes are a necessary cellular element for pathogenesis in both GKO and WT genotypes.

Materials and Methods

Animals

Mice with a targeted disruption of the interferon-γ gene (GKO mice) and WT C57BL/6 control mice were obtained from the Jackson Laboratory (Bar Harbor, ME). The mice were housed in

specific pathogen-free conditions and were used at 8 to 12 weeks of age. The use of the animals conformed to the ARVO Statement for the Use of Animals in Ophthalmic and Vision Research.

Antigen and Reagents

Complete Freund's adjuvant (CFA) was purchased from Difco (Detroit, MI); *Mycobacterium tuberculosis* strain H37RA (MTB) from Sigma-Aldrich (St. Louis, MO); and purified *Bordetella* pertussis toxin (PT) from Sigma-Aldrich. IRBP was isolated from bovine retinas, as described previously, by using Con A-sepharose affinity chromatography and fast-performance liquid chromatography.[30] IRBP preparations were aliquoted and stored at −70° C.

EAU Induction and Scoring

EAU was induced by immunization with 150 μg of IRBP in phosphate-buffered saline (PBS) emulsified 1:1 vol/vol in complete Freund's adjuvant (CFA) that had been supplemented with MTB to 2.5 mg/mL. A total of 200 μL emulsion was injected subcutaneously, divided among the base of the tail and both thighs. PT (0.5 μg/mouse) in PBS containing 2% normal mouse serum was given by intraperitoneal injection concurrently with immunization. Clinical EAU was evaluated by funduscopy under a binocular microscope after dilation of the pupil and was graded on a scale of 0 to 4, according to criteria based on the extent of inflammatory lesions, as described in detail elsewhere.[31] Eyes harvested 21 days after immunization were prefixed in 4% phosphatebuffered glutaraldehyde for 1 hour (to prevent artifactual detachment of the retina) and then were transferred to 10% phosphate-buffered formaldehyde until processing. Fixed and dehydrated tissue was embedded in methacrylate, and 4- to 6-μm sections were stained with standard hematoxylin and eosin. Eye sections cut through the pupillary optic nerve plane were scored in a masked fashion. Severity of EAU was graded on a scale of 0 to 4 in half-point increments according to criteria described previously, based on the type, number, and size of lesions.[31,32]

RNA Isolation

Total RNA was extracted from the lymph nodes and eyes of mice immunized with IRBP at the indicated time points (Atlas Pure Total RNA kit; BD-Clontech, Palo Alto, CA). RNA samples were treated with DNase to remove traces of genomic DNA and were quantified by spectrophotometric analysis. The ratios of A_{260}/A_{280} of the samples were higher than 1.8. The samples were checked for integrity using formaldehyde denaturing RNA gel electrophoresis (1.2%) before proceeding with the further microarray and real-time PCR analysis.

Microarrays and Data Analysis

Two micrograms of total RNA from each time point were labeled (SuperArray Ampolabeling Linear Polymerase Reaction [LPR] kit; SuperArray Bioscience Corp., Frederick, MD), according to the manufacturer's protocol. Hybridization was performed on 128 sites (114 genes and 14 blank or reference spots) (Oligo GEArray Mouse Chemokines and Receptors Microarray; OMM-022, SuperArray Bioscience Corp.; Frederick, MD) according to the manufacturer's protocol. The chemiluminescent signals were captured by charge-coupled device (CCD) camera equipment (LAS-1000, Diana; Fujufilm, Valhalla, NY). Data were extracted and analyzed with gene expression analysis (GEArray suite; Syngene, Ltd., Frederick, MD). Background-corrected signals were normalized to the averaged intensity of signals for the control genes by using the manufacturer's software (Syngene, Ltd.).

Real-Time RT-PCR

cDNA synthesis was performed with 2 μg of the same RNA that was used for microarray hybridization using a SYBR green–based PCR kit (Advantage RT-for PCR; BD-Clontech) in

a final volume of 20 μL, according to the manufacturer's protocol. cDNA reactions were incubated at 70°C for 10 minutes to denature the RNA template and were quench-cooled for 5 minutes. AMV reverse transcriptase was added, and reactions were incubated at 42°C for 60 minutes. cDNA reactions were diluted 1:10, and 5 μL of the diluted cDNA reaction was added to a 45-μL PCR solution containing 0.5 μM of each primer and SYBR green master mix in 96-well plates (Brilliant SYBR Green QOCR; Stratagene, La Jolla, CA). The PCR reactions were then performed (MX3000p system; Stratagene), with the system set to work with the SYBR green–determination program with a 10-minute initial hot-start activation of the *Taq* polymerase at 95°C, followed by 40 cycles of amplification (95°C for 10 seconds, 56°C for 5 seconds, and 72°C for 10 seconds). After amplification, a melting curve was generated by holding the reaction at 65°C for 15 seconds and then heating to 95°C with a ramp rate of 0.1° C/s. To give melting temperature for each sample, the fluorescence signal was plotted against temperature. The comparative CT (threshold cycle) method normalized to GAPDH was used to analyze relative changes in gene expression as previously described[33] (amount of target = $2^{-\Delta\Delta CT}$).

Cytokine Assays

For analysis of tissue culture supernatants, inguinal and iliac lymph node cells from immunized mice were cultured in 24-well flat-bottomed plates (5×10^6 cells/1 mL culture medium per well) with or without IRBP at 20 μg/mL. Supernatants were collected after 48 hours and were kept frozen in small aliquots at −70°C. For eye extract, both left and right eyes enucleated from five WT or five GKO mice at the indicated time points after IRBP immunization in 300 μL of PBS with proteinase inhibitor cocktails (Calbiochem-EMD, San Diego, CA) were minced with scissors into small pieces, and then the tissue was disrupted by gentle sonication. Soluble fraction was collected after high-speed centrifugation. All procedures were performed at 4°C. Cytokine and chemokine protein levels in the supernatants and eye extracts were measured by multiplex ELISA (SearchLight technology; Pierce Boston Technology, Woburn, MA)[34] (http://www.searchlightonline.com) or by single cytokine ELISA kits from R&D systems (CCL22, CXCL2, CXCL9, and CXCL10).

In Vivo Depletion of Eosinophils with Anti-CCR3 or Depletion of Granulocytes with Anti-GR–1 Monoclonal Antibodies

EAU in WT and GKO mice was induced by immunization with IRBP in CFA on day 0 as described earlier. For eosinophil depletion, the mice were injected IP with 0.5 mg purified rat anti-mouse CCR3 monoclonal antibody (clone 6S2-19-4; IgG2b; kindly provided by Robert L. Coffman, at the time at DNAX Inst., Palo Alto, CA currently at Dynavax Technol. Corp., Berkeley, CA) or isotype control antibody (SFR8-B6, purchased from ATCC) daily from day 1 to day 13. For granulocyte depletion, the mice were injected IP with 100 μg rat anti-mouse GR-1 monoclonal antibody (clone RB6-8C5, IgG2b isotype) or isotype control antibody (SFR8-B6) on days −1, 3, 6, 9, 12, and 15. On day 18, 300 to 500 μL of peripheral blood was collected from randomly selected mice for complete blood counts (CBCs) to examine the specificity of the antibodies. The CBCs showed that treatment with anti-CCR3 depleted eosinophils only. The anti-Gr-1 antibody depleted neutrophils, eosinophils, and basophiles with an efficiency greater than 95%. At this treatment dose, the monocyte and lymphocyte counts remained within normal range (Table 1). Clinical EAU was scored by funduscopy on days 14 and 19 and was confirmed by histopathology in eyes collected on day 21 after immunization.

Reproducibility and Statistical Analysis

Experiments were repeated at least twice, usually three or more times. Results were highly reproducible. Figures show pooled data from repeat experiments, or representative

experiments, as indicated. Each point is one mouse (average of both eyes). Statistical significance of differences in disease scores was calculated using Snedecor and Cochran's test for linear trend in proportions.[35] This is a nonparametric test that generates its probabilities by frequency analysis of the number of individuals at each possible score, thus taking into account both severity and incidence of disease. Each mouse (average of both eyes) was treated as one statistical event. DTH and lymphocyte proliferation data were analyzed by using student's independent *t*-test. $P \leq 0.05$ was considered significant.

Results

Clinical and Histologic Features of EAU in WT and GKO Mice

EAU was induced in GKO mice on the C57BL/6 background and in WT C57BL/6 control mice by immunization with the retinal antigen IRBP as described in the Materials and Methods section. C57BL/6 mice are a moderately susceptible strain and typically have low disease scores. However, histopathology of eyes collected 21 days after immunization revealed that GKO mice developed considerably more severe EAU as compared their WT control animals (Fig. 1A). Their immune responses including DTH and T-lymphocyte proliferation were also higher than in WT control mice (Figs. 1B, 1C). Analysis of the cellular composition of the ocular inflammatory infiltrates revealed that infiltrating cells in WT mice were mononuclear cells, including T cells and monocytes, with a few neutrophils. However, infiltrating cells in the eyes of GKO mice were mainly granulocytes, including neutrophils and eosinophils, with a relative paucity of lymphocytes and monocytes (Fig. 2). These data are in line with our previous observations in EAU-challenged GKO and WT mice.[15,17]

Gene Expression Analysis in WT and GKO Mice

Next, we examined the expression of chemokines that might account for the different cell populations infiltrating the eyes in WT and GKO mice. Oligonucleotide arrays specific for mouse chemokines were used to screen genes differentially expressed during EAU development in WT and GKO mice. RNA extraction, microarray, and data analysis were performed as described in the Materials and Methods section. The intensity of each chemokine signal in eyes of naïve WT mice was similar to the gene in GKO mice (data not shown). Several chemokine genes were differentially upregulated in uveitic eyes and in lymph nodes from IRBP immunized animals (Table 1). In eyes analyzed within 1 day of clinical onset of disease, expression of the genes for CCL1, CCL2, CCL17, CCL21, CCL22, CCL24, CXCL10, and CXCL9 in both WT and GKO mice was upregulated compared with baseline in naïve mice. However, CCL5 and CXCL11 were upregulated only in WT mice, whereas CCL11, CCL3, CCL7, CXCL15, and CXCL2 were increased only in GKO mice. The signals for CCL5, CXCL10, CXCL11, and CXCL9 in WT mice were markedly higher than in GKO mice (ratio, >1.5). In contrast, the intensity of CCL1, CCL11, CCL17, CCL22, and CCL3 in GKO mice was stronger than that in WT mice (Table 1). We also examined the chemokine mRNA expression in lymph nodes. Similar to normal eyes, each gene expression in both lymph nodes from normal WT and GKO animals was similar intensity (data not shown). In lymph nodes taken 3 days after IRBP immunization—thought mostly to represent the innate response to CFA—CXCL10, CXCL11, CCL5, CXCL9, CXCL4, CCL9, and CCL2 in WT mice and CCL11, CCL1, CCL21, CCL22, CCL24, and CCL7 in GKO mice were upregulated (Table 1). We next examined chemokine expression by Ag-stimulated draining lymph node cells from IRBP-immunized animals collected 21 days after immunization, which represents the adaptive response. In WT mice, genes for CCL5, CCL8, CCL9, CXCL10, CXCL11, and CXCL9 in lymph node cells were upregulated, whereas in GKO mice CCL1, CCL17, CCL21, CCL22 and CXCL2 were upregulated (Table 2).

Real-time PCR was used to verify the data obtained from array analysis. Table 3 shows the specific primers for the chemokines that were tested. Figures 3A and 3B show changes in chemokine genes during EAU development. In naïve mice, the baseline expression level of all chemokines tested in eyes and in lymph nodes was similar in WT and GKO mice (Figs. 3A, 3C). However, in eyes at onset of disease the mRNA transcripts for most chemokine genes were markedly increased in both WT and GKO mice. CXCL10, CXCL11, CXCL9, CCL5, and CCL2 were higher in WT mice than in GKO mice whereas CCL11, CCL22, CCL17, CCL1, CCL3, and CCL21 were higher in GKO mice than in WT mice (Fig. 3B). In lymph nodes from naive WT mice and GKO mice, the basal expression of most genes was low and was similar in both genotypes, except for CCL5 which was expressed in WT more highly than in GKO, with the converse being observed for CCL21 (Fig. 3C). We next examined expression of chemokine genes in draining lymph nodes 3 days after immunization (mostly innate response to adjuvant), by direct ex vivo analysis. Similar to the gene expression pattern in eyes, many genes were upregulated in lymph nodes 3 days after IRBP immunization, with CXCL10, CXCL9, CCL5, and CCL2 higher in WT and CCL11, CCL22, CCL17, CCL1, and CCL21 higher in GKO (Fig. 3D). Analysis of the adaptive response (lymph nodes explanted into culture 21 days after immunization and stimulated with IRBP) revealed that lymph node cells from WT mice again expressed higher CXCL10, CXCL9, and CCL5 compared with the levels in GKO mice. Lymph node cells from GKO mice expressed higher CCL11, CCL22, CCL17, CCL1, CCL21, and CXCL2 (Fig. 3F). Thus, the measurements of chemokine message expression by real-time PCR are consistent with the data obtained by microarray analysis.

Protein Levels of Chemokines during EAU Development

We next analyzed the protein levels of the chemokines differentially regulated according to the data obtained by microarray and real-time PCR. The protein concentration in extracts of eyes from WT and GKO mice 13 days (1 day after EAU onset) or 21 days (fully developed EAU) after IRBP-immunization was measured by ELISA. Substantially increased CXCL10, CXCL9, and CCL5 were observed in WT mice. Whereas, CCL11, CCL22, CCL17, and CXCL2 were dominant in the eyes in GKO mice (Fig. 4A). We also measured the level of these chemokines in culture supernatants of lymph node cells from IRBP-immunized mice, to correspond to the adaptive response evaluation by real-time PCR. Lymph node cells from WT mice secreted large amounts of CXCL10, CXCL9, and CCL5 whereas lymph node cells from GKO mice produced CCL22, CCL17, and CXCL2 after antigen stimulation (Fig. 4B), in agreement with RNA analysis data. Unlike the RNA data, CCL11 protein secretion by lymph node cells was low (Fig. 4B). This discrepancy may be due to posttranscriptional effects' preventing synthesis of protein in the culture system.

Kinetics of Disease Development and Inflammatory Cell Composition in WT and GKO Mice

Next, we examined kinetics of disease and composition of the ocular inflammatory infiltrate in WT and GKO mice. All mice were immunized with IRBP in CFA as described in the Materials and Methods section. Clinical EAU was monitored by fundus examination under a binocular microscope at 2, 3, 4, and 5 weeks after immunization (Fig. 5). Although disease scores were higher in GKO mice, both GKO and WT reached their respective peak scores between weeks 2 and 3. Disease receded thereafter, nearing resolution of active inflammation by week 5 (Fig. 5).

The composition of inflammatory infiltrate was examined in histologic sections stained with hematoxylin and eosin (Table 4). Early in the disease, WT mice showed a typical mononuclear infiltrate that was essentially preserved throughout the disease course, in which lymphocytes and monocytes together accounted for approximately 80% of the infiltrating cells, with the remaining 20% composed largely of neutrophils. In contrast, over 60% of the infiltrate in GKO at EAU onset was composed of granulocytes with a prominent eosinophilic component. The

proportion of granulocytes in eyes of GKO mice was reduced as active disease neared resolution.

Effect of Depletion of Granulocytes or of Eosinophils only, on EAU Development

Granulocytes, containing a substantial proportion of eosinophils, constitute a dominant infiltrating population in GKO mice (Fig. 1 and Refs. 15,17). We therefore examined whether these cells are functionally important in EAU pathogenesis, and whether depletion of these cells would abrogate disease. GKO mice and WT controls were treated either with anti-CCR3 monoclonal Ab to deplete eosinophils or with anti-Gr-1 monoclonal Ab, which results in depletion of all granulocyte types. CBCs showed >95% depletion of the target populations but no apparent effect on other leukocyte types (Table 1). Immunization of depleted mice for EAU showed that depletion of eosinophils alone did not protect from disease in either WT or GKO mice (Fig. 6A). The infiltrating cells in eyes of GKO mice after anti-CCR3 treatment contained few if any eosinophils, but overall disease scores were not affected. In contrast, depletion of all granulocytes abrogated development of disease in both WT and GKO mice (Fig. 6B). Thus, it appears that neutrophils, but not eosinophils, are critical cells for development of histopathology in EAU in GKO mice, as well as in WT mice, where they do not constitute the numerically dominant population.

Discussion

Previous studies from our laboratory indicated that, despite findings implicating Th1-like cells in the pathogenesis of EAU and the Th1-dominant response phenotype in susceptibility to the disease, systemically produced IFN-γ in fact appears to limit EAU and immunologic responses to IRBP. This notion is supported by the observation that the treatment of EAU-susceptible mice with neutralizing anti-IFN-γ antibody exacerbates EAU and antigen-specific DTH[14] and by the higher susceptibility to EAU and elevated immunologic responses of the GKO mouse.[15,17] Excess IFN-γ, whether administered directly or induced by IL-12 treatment, protects against EAU.[14,36] Induction of more severe disease in GKO mice and/or IFN-γ receptor KO mice has also been reported in the model of experimental allergic encephalomyelitis (EAE),[37,38] collagen-induced arthritis,[39,40] and experimental autoimmune thyroiditis (EAT).[41] These diseases were typically accompanied by upregulation of IL-5, IL-6, and IL-10 in GKO mice, a Th2-like cytokine response profile.[15,17] Recent data from our laboratory reveal that GKO mice also have increased expression of IL-17 both systemically and locally in the eye, that is typically two to three times higher than in the corresponding WT controls (Ref. 42 and Luger D et al., manuscript submitted).

A typical feature of the GKO disease is heavy infiltration of granulocytes, with prominent participation of eosinophils, into the target tissue (Fig. 2 and Refs. 15,17). We have now shown that in the presence of an IFN-γ response, the chemoattractants for Th1-polarized cells, CXCL9, CXCL10, CXCL11, CCL5, and infiltrating mononuclear cells predominate in EAU eyes, whereas in its absence, Th2-associated chemoattractants, CCL11, CCL17, CCL1, and Th17-associated chemokines CCL22 and CXCL2, prevail during EAU development. Thus, IFN-γ acts as a primary regulator of chemokine profiles and influences the autoimmune inflammatory response in the WT mouse at least in part by restricting infiltration of neutrophils and eosinophils, whose increased presence may underlie the more severe EAU pathology seen in GKO mice.

Our finding that IFN-γ drives production of CXCL10, CXCL9, CCL5, and CXCL11 in EAU is consistent with data in other autoimmune diseases. However, our characterization is much more extensive than what was done in these earlier studies. In the EAE model, CXCL10 and CXCL11 were reported to be significantly elevated,[43,44] and were low in GKO mice.[45] Klimiuk et al.[46] reported that CCL5 was increased in patients with rheumatoid arthritis. Patients

with myasthenia gravis express high levels of CXCL10 and CXCL9.[47] One of the known effects of IFN-γ is to suppress the development of Th2 cytokines, and it has recently been reported to do the same for IL-17.[11] Thus, EAU and EAT, both normally Th1-mediated diseases, become biased in GKO mice toward a Th2- and Th17- like response.[15,41,42] IFN-γ is therefore a key cytokine in coordinating the expression of local autoimmune and inflammatory responses.

In the absence of IFN-γ, the chemokines CCL11, CCL22, CCL17, CCL1, and CXCL2 predominate and appear to act as inducers of the invasion of the eye by neutrophils and eosinophils. These chemokines also play an important role in other autoimmune diseases. Hessner et al.[48] reported that CCL11 was involved in the development of type 1 diabetes mellitus in the BioBreeding (BB) rat. CCL11 was overexpressed in lesions of patients with pemphigoid gestationis,[49] and bullous pemphigoid. [50] CCL17 and CCL22 were elevated in the patients with pulmonary fibrosis, systemic sclerosis, and systemic lupus erythematosus.[22,51,52] CCL1 was upregulated in chronic relapsing EAE[53] and in atopic dermatitis.[54] The other chemokine CXCL2, the functionally analogous to human IL-8, may also act on the migration of neutrophils. However, chemokine protein analysis showed a marked increase of CXCL2 in recent-onset eyes in GKO mice, suggesting that this chemokine may play a critical role in the regulation of neutrophil infiltration in GKO mice.

We did not attempt to identify the cellular sources of the chemokines measured in the eye. The finding that immune lymph node cells from WT mice produced large amounts of CXCL10, CXCL9, and CCL5, while $CD4^+$ T cells from GKO mice produced mainly CCL22, CCL17, and CXCL2, in similarity to the expression profile within the eye during uveitis, suggests that antigen-specific T cells recruited into the eye are at least one of the local sources of chemokines. However, resident retinal cells in the eye have been shown to produce chemokines and undoubtedly contribute to the observed profile (reviewed in Wallace et al.[55]). Finally, non-Ag specific leukocytes recruited from the circulation may also be a source of chemokines within the eye.

The predominance of granulocytes in the ocular infiltrate in GKO mice could not be explained by a general excess of granulocytes in these mice, as CBCs in GKO and WT mice showed that the total leukocyte count and the absolute number of neutrophils, lymphocytes, monocytes, eosinophils, and basophils were similar (data not shown). Thus, the predominance of granulocytes in the inflammatory infiltrate must represent specific recruitment. Granulocytes appear to have an important functional role in the pathology of EAU. Depletion of total granulocytes, but not of eosinophils only (despite their relative prominence in the inflammatory infiltrate), abrogated EAU development, suggesting a nonredundant role for neutrophils rather than eosinophils in the pathogenesis of EAU. Notably, disease was abrogated not only in GKO mice, where granulocytes constitute a dominant population, but also in WT mice where they do not. This indicates that even though they are a minor proportion of the infiltrating cells, granulocytes contribute decisively to disease, which was not previously recognized in the uveitis model. The large predominance of granulocytes in GKO mice could explain the higher disease scores typical of this genotype. Our data are in line with the report of McColl et al.,[56] who reported that depletion of granulocytes by monoclonal antibody treatment inhibits the effector phase of MBP-induced EAE in SJL/J mice and MOG-induced EAE in IFN-γ receptor–deficient mice. The critical role of granulocytes in disease that affects neural tissue (i.e., retina and brain), suggests that chemokines or chemokine receptors involved in recruitment of these cells may constitute targets for local anti-inflammatory therapy.

Acknowledgments

Supported by the National Institutes of Health Intramural Program.

References

1. Gery I, Mochizuki M, Nussenblatt RB. Retinal specific antigens and immunopathogenic processes they provoke. Prog Retinal Res 1986;5:75–109.
2. Caspi RR, Roberge FG, Chan CC, et al. A new model of autoimmune disease: experimental autoimmune uveoretinitis induced in mice with two different retinal antigens. J Immunol 1988;140:1490–1495. [PubMed: 3346541]
3. Wacker WB, Donoso LA, Kalsow CM, Yankeelov JA Jr, Organisciak DT. Experimental allergic uveitis: isolation, characterization, and localization of a soluble uveitopathogenic antigen from bovine retina. J Immunol 1977;119:1949–1958. [PubMed: 334977]
4. Faure JP. Autoimmunity and the retina. Curr Top Eye Res 1980;2:215–302. [PubMed: 7344837]
5. Nussenblatt, RB.; Whitcup, SM.; Palestine, AG. Uveitis: Fundamentals and Clinical Practice. Vol. 2. St. Louis: Mosby Year Book, Inc; 1996. p. 22-26.
6. Mosmann TR, Cherwinski H, Bond MW, Giedlin MA, Coffman RL. Two types of murine helper T cell clone. I. Definition according to profiles of lymphokine activities and secreted proteins. J Immunol 1986;136:2348–2357. [PubMed: 2419430]
7. Mosmann TR, Coffman RL. TH1 and TH2 cells: different patterns of lymphokine secretion lead to different functional properties. Annu Rev Immunol 1989;7:145–173. [PubMed: 2523712]
8. Romagnani S. Lymphokine production by human T cells in disease states. Annu Rev Immunol 1994;12:227–257. [PubMed: 8011282]
9. O'Garra A. Cytokines induce the development of functionally heterogeneous T helper cell subsets. Immunity 1998;8:275–283. [PubMed: 9529145]
10. Kim YK, Myint AM, Lee BH, et al. Th1, Th2 and Th3 cytokine alteration in schizophrenia. Prog Neuropsychopharmacol Biol Psychiatry 2004;28:1129–1134. [PubMed: 15610925]
11. Wynn TA. T(H)-17: a giant step from T(H)1 and T(H)2. Nat Immunol 2005;6:1069–1070. [PubMed: 16239919]
12. Park H, Li Z, Yang XO, et al. A distinct lineage of CD4 T cells regulates tissue inflammation by producing interleukin 17. Nat Immunol 2005;6:1133–1141. [PubMed: 16200068]
13. Harrington LE, Hatton RD, Mangan PR, et al. Interleukin 17-producing CD4+ effector T cells develop via a lineage distinct from the T helper type 1 and 2 lineages. Nat Immunol 2005;6:1123– 1132. [PubMed: 16200070]
14. Caspi RR, Chan CC, Grubbs BG, et al. Endogenous systemic IFN-gamma has a protective role against ocular autoimmunity in mice. J Immunol 1994;152:890–899. [PubMed: 8283058]
15. Jones LS, Rizzo LV, Agarwal RK, et al. IFN-gamma-deficient mice develop experimental autoimmune uveitis in the context of a deviant effector response. J Immunol 1997;158:5997–6005. [PubMed: 9190954]
16. Tran EH, Prince EN, Owens T. IFN-gamma shapes immune invasion of the central nervous system via regulation of chemokines. J Immunol 2000;164:2759–2768. [PubMed: 10679118]
17. Avichezer D, Chan CC, Silver PB, Wiggert B, Caspi RR. Residues 1-20 of IRBP and whole IRBP elicit different uveitogenic and immunological responses in interferon gamma deficient mice. Exp Eye Res 2000;71:111–118. [PubMed: 10930316]
18. Campbell JJ, Butcher EC. Chemokines in tissue-specific and microenvironment- specific lymphocyte homing. Curr Opin Immunol 2000;12:336–341. [PubMed: 10781407]
19. Stein JV, Nombela-Arrieta C. Chemokine control of lymphocyte trafficking: a general overview. Immunology 2005;116:1–12. [PubMed: 16108812]
20. Shimada Y, Takehara K, Sato S. Both Th2 and Th1 chemokines (TARC/CCL17, MDC/CCL22, and Mig/CXCL9) are elevated in sera from patients with atopic dermatitis. J Dermatol Sci 2004;34:201–208. [PubMed: 15113590]
21. Liu L, Jarjour NN, Busse WW, Kelly EA. Enhanced generation of helper T type 1 and 2 chemokines in allergen-induced asthma. Am J Respir Crit Care Med 2004;169:1118–1124. [PubMed: 15001464]
22. Belperio JA, Dy M, Murray L, et al. The role of the Th2 CC chemokine ligand CCL17 in pulmonary fibrosis. J Immunol 2004;173:4692–4698. [PubMed: 15383605]

23. Ley K, Smith E, Stark MA. IL-17A-producing neutrophil-regulatory Tn lymphocytes. Immunol Res 2006;34:229–242. [PubMed: 16891673]
24. Kikly K, Liu L, Na S, Sedgwick JD. The IL-23/Th(17) axis: therapeutic targets for autoimmune inflammation. Curr Opin Immunol 2006;18:670–675. [PubMed: 17010592]
25. Crane IJ, McKillop-Smith S, Wallace CA, Lamont GR, Forrester JV. Expression of the chemokines MIP-1alpha, MCP-1, and RANTES in experimental autoimmune uveitis. Invest Ophthalmol Vis Sci 2001;42:1547–1552. [PubMed: 11381059]
26. Keino H, Takeuchi M, Kezuka T, Yamakawa N, Tsukahara R, Usui M. Chemokine and chemokine receptor expression during experimental autoimmune uveoretinitis in mice. Graefes Arch Clin Exp Ophthalmol 2003;241:111–115. [PubMed: 12605265]
27. Foxman EF, Zhang M, Hurst SD, et al. Inflammatory mediators in uveitis: differential induction of cytokines and chemokines in Th1-versus Th2-mediated ocular inflammation. J Immunol 2002;168:2483–2492. [PubMed: 11859142]
28. Fife BT, Kennedy KJ, Paniagua MC, et al. CXCL10 (IFN-gamma-inducible protein-10) control of encephalitogenic CD4+ T cell accumulation in the central nervous system during experimental autoimmune encephalomyelitis. J Immunol 2001;166:7617– 7624. [PubMed: 11390519]
29. Su SB, Silver PB, Zhang M, Chan CC, Caspi RR. Pertussis toxin inhibits induction of tissue-specific autoimmune disease by disrupting G protein-coupled signals. J Immunol 2001;167:250–256. [PubMed: 11418656]
30. Pepperberg DR, Okajima TL, Ripps H, Chader GJ, Wiggert B. Functional properties of interphotoreceptor retinoid-binding protein. Photochem Photobiol 1991;54:1057–1060. [PubMed: 1775528]
31. Caspi, RR. Experimental autoimmune uveoretinitis (EAU): mouse and rat. In: Coligan, JE.; Kruisbeek, AM.; Margulies, DH.; Shevach, EM.; Strober, W., editors. Current Protocols in Immunology. Vol. 3. New York: John Wiley & Sons; 2003.
32. Chan CC, Caspi RR, Ni M, et al. Pathology of experimental autoimmune uveoretinitis in mice. J Autoimmun 1990;3:247–255. [PubMed: 2397018]
33. Livak KJ, Schmittgen TD. Analysis of relative gene expression data using real-time quantitative PCR and the 2(−Delta Delta C(T)) Method. Methods 2001;25:402–408. [PubMed: 11846609]
34. Moody MD, Van Arsdell SW, Murphy KP, Orencole SF, Burns C. Array-based ELISAs for high-throughput analysis of human cytokines. BioTechniques 2001;31:186–190. 192–184. [PubMed: 11464511]
35. Snedecor, GW.; Cochran, WG. Statistical Methods. Ames, IA: Iowa State University Press; 1967.
36. Tarrant TK, Silver PB, Wahlsten JL, et al. Interleukin 12 protects from a T helper type 1-mediated autoimmune disease, experimental autoimmune uveitis, through a mechanism involving interferon gamma, nitric oxide, and apoptosis. J Exp Med 1999;189:219– 230. [PubMed: 9892605]
37. Ferber IA, Brocke S, Taylor-Edwards C, et al. Mice with a disrupted IFN-gamma gene are susceptible to the induction of experimental autoimmune encephalomyelitis (EAE). J Immunol 1996;156:5–7. [PubMed: 8598493]
38. Krakowski M, Owens T. Interferon-gamma confers resistance to experimental allergic encephalomyelitis. Eur J Immunol 1996;26:1641–1646. [PubMed: 8766573]
39. Manoury-Schwartz B, Chiocchia G, Bessis N, et al. High susceptibility to collagen-induced arthritis in mice lacking IFN-gamma receptors. J Immunol 1997;158:5501–5506. [PubMed: 9164973]
40. Vermeire K, Heremans H, Vandeputte M, Huang S, Billiau A, Matthys P. Accelerated collagen-induced arthritis in IFN-gamma receptor-deficient mice. J Immunol 1997;158:5507–5513. [PubMed: 9164974]
41. Tang H, Sharp GC, Peterson KP, Braley-Mullen H. IFN-gamma-deficient mice develop severe granulomatous experimental autoimmune thyroiditis with eosinophil infiltration in thyroids. J Immunol 1998;160:5105–5112. [PubMed: 9590262]
42. Tang J, Zhu W, Silver PB, Su SB, Chan CC, Caspi RR. Autoimmune uveitis elicited with antigen-pulsed dendritic cells has a distinct clinical signature and is driven by unique effector mechanisms: initial encounter with autoantigen defines disease phenotype. J Immunol 2007;178:5578–5587. [PubMed: 17442940]

43. Klein RS, Izikson L, Means T, et al. IFN-inducible protein 10/CXC chemokine ligand 10-independent induction of experimental autoimmune encephalomyelitis. J Immunol 2004;172:550–559. [PubMed: 14688366]
44. McColl SR, Mahalingam S, Staykova M, et al. Expression of rat I-TAC/CXCL11/SCYA11 during central nervous system inflammation: comparison with other CXCR3 ligands. Lab Invest 2004;84:1418– 1429. [PubMed: 15322564]
45. Glabinski AR, Krakowski M, Han Y, Owens T, Ransohoff RM. Chemokine expression in GKO mice (lacking interferon-gamma) with experimental autoimmune encephalomyelitis. J Neurovirol 1999;5:95–101. [PubMed: 10190695]
46. Klimiuk PA, Sierakowski S, Latosiewicz R, et al. Histological patterns of synovitis and serum chemokines in patients with rheumatoid arthritis. J Rheumatol 2005;32:1666–1672. [PubMed: 16142858]
47. Feferman T, Maiti PK, Berrih-Aknin S, et al. Overexpression of IFN-induced protein 10 and its receptor CXCR3 in myasthenia gravis. J Immunol 2005;174:5324–5331. [PubMed: 15843529]
48. Hessner MJ, Wang X, Meyer L, et al. Involvement of eotaxin, eosinophils, and pancreatic predisposition in development of type 1 diabetes mellitus in the BioBreeding rat. J Immunol 2004;173:6993–7002. [PubMed: 15557196]
49. Gunther C, Wozel G, Dressler J, Meurer M, Pfeiffer C. Tissue eosinophilia in pemphigoid gestationis: association with eotaxin and upregulated activation markers on transmigrated eosinophils. Am J Reprod Immunol 2004;51:32–39. [PubMed: 14725564]
50. Frezzolini A, Teofoli P, Cianchini G, et al. Increased expression of eotaxin and its specific receptor CCR3 in bullous pemphigoid. Eur J Dermatol 2002;12:27–31. [PubMed: 11809592]
51. Fujii H, Shimada Y, Hasegawa M, Takehara K, Sato S. Serum levels of a Th1 chemoattractant IP-10 and Th2 chemoattractants, TARC and MDC, are elevated in patients with systemic sclerosis. J Dermatol Sci 2004;35:43–51. [PubMed: 15194146]
52. Okamoto H, Koizumi K, Yamanaka H, Saito T, Kamatani N. A role for TARC/CCL17, a CC chemokine, in systemic lupus erythematosus. J Rheumatol 2003;30:2369–2373. [PubMed: 14677179]
53. Glabinski AR, Bielecki B, Ransohoff RM. Chemokine upregulation follows cytokine expression in chronic relapsing experimental autoimmune encephalomyelitis. Scand J Immunol 2003;58:81– 88. [PubMed: 12828562]
54. Gombert M, Dieu-Nosjean MC, Winterberg F, et al. CCL1–CCR8 interactions: an axis mediating the recruitment of T cells and Langerhans-type dendritic cells to sites of atopic skin inflammation. J Immunol 2005;174:5082–5091. [PubMed: 15814739]
55. Wallace GR, John Curnow S, Wloka K, Salmon M, Murray PI. The role of chemokines and their receptors in ocular disease. Prog Retin Eye Res 2004;23:435–448. [PubMed: 15219876]
56. McColl SR, Staykova MA, Wozniak A, Fordham S, Bruce J, Willenborg DO. Treatment with anti-granulocyte antibodies inhibits the effector phase of experimental autoimmune encephalomyelitis. J Immunol 1998;161:6421–6426. [PubMed: 9834134]

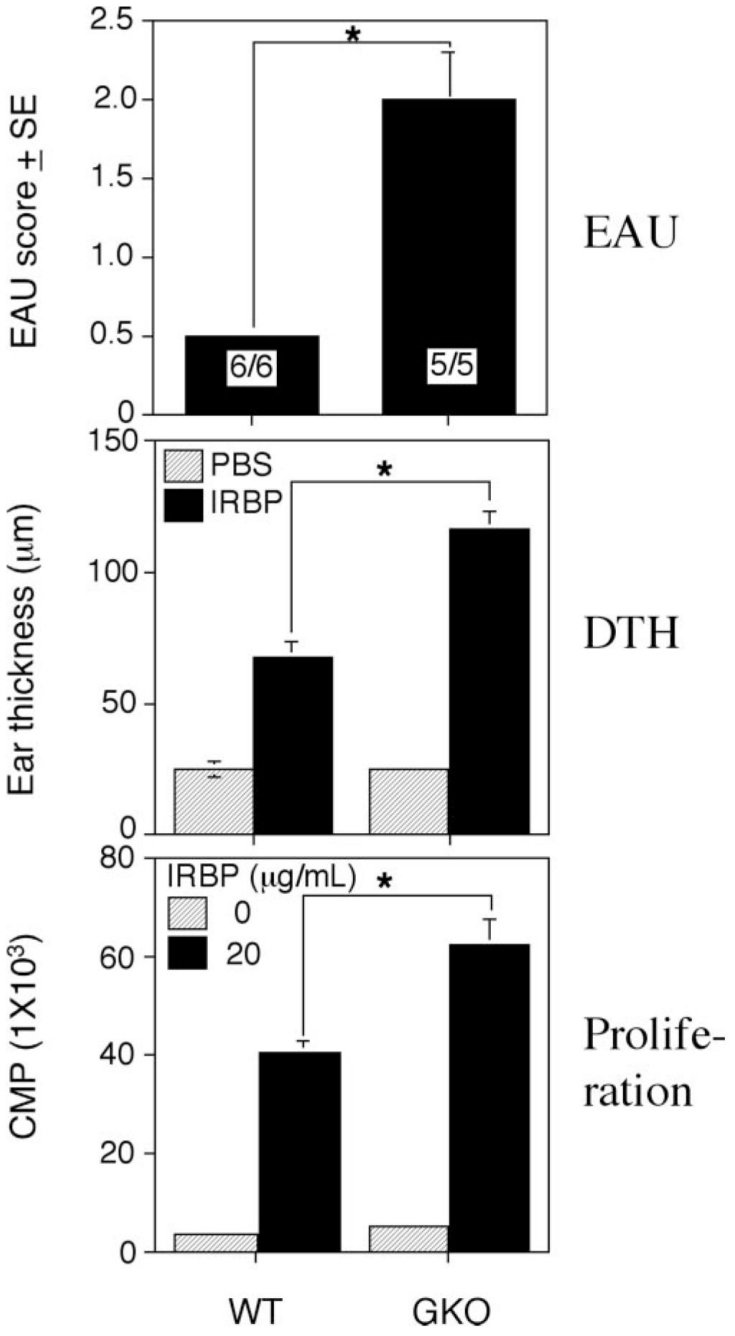

Figure 1.

EAU and related immune responses in WT and GKO mice. GKO and control WT mice were immunized with 150 μg IRBP emulsified in CFA and received 0.5 μg of PT IP. (**A**) The EAU score was evaluated by histopathology at 21 days after immunization. The EAU score is the average of all the mice in the group. EAU incidence (positive/total) is shown in each bar. Shown is a representative experiment of three. (**B**) DTH responses were elicited on day 19 and were evaluated on day 21 after immunization. (**C**) Ag-specific proliferation of lymph nodes from immunized mice was determined by incorporation of [^{3}H]thymidine. Shown are counts per minute from one representative experiment of three (average of triplicates). *Statistically significant difference in scores versus WT ($P < 0.05$).

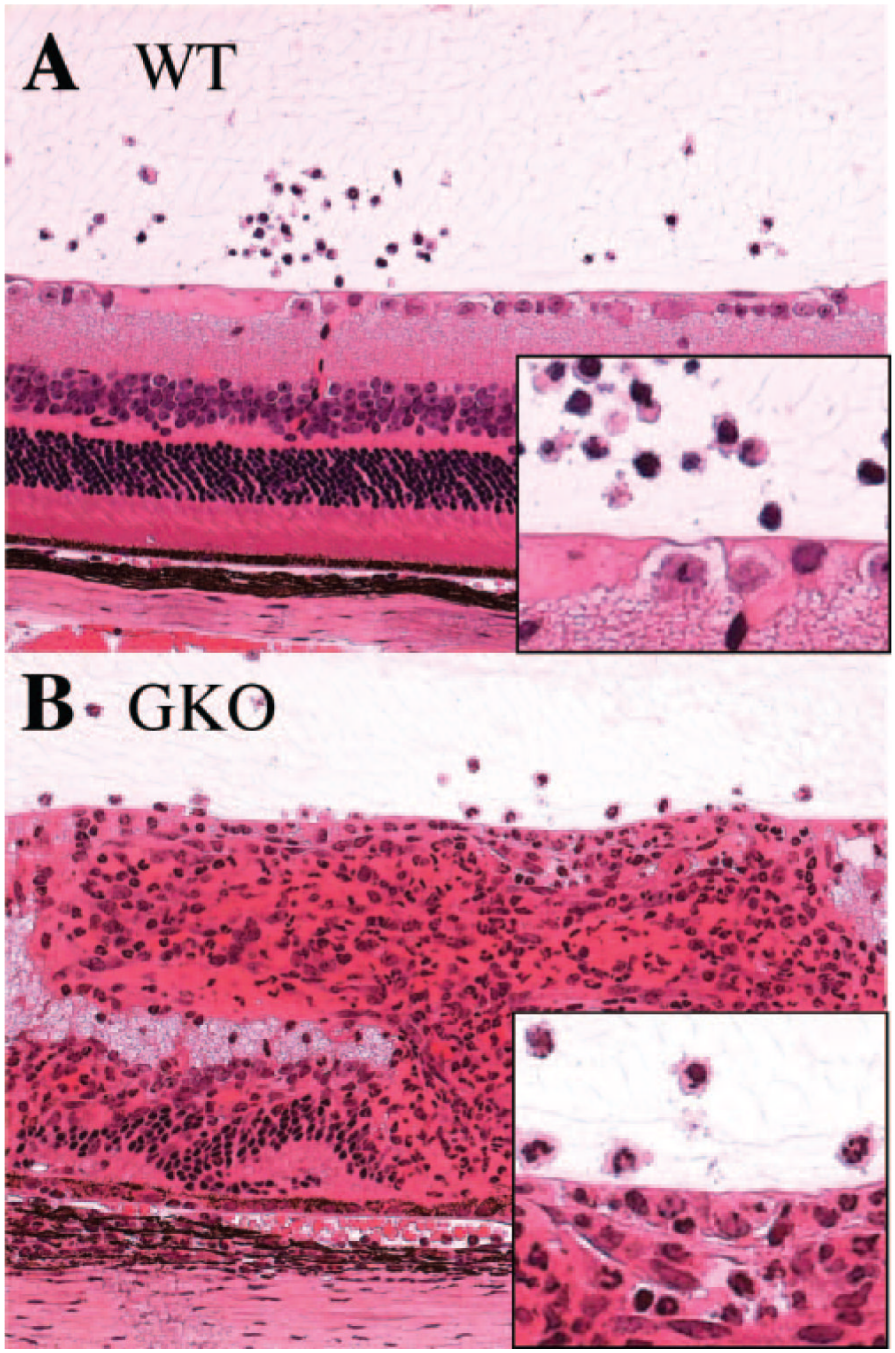

Figure 2.
Ocular histopathology of WT and GKO mice. (**A**) EAU (score, 0.5) in WT mice with mononuclear cell infiltration. (**B**) EAU (score, 2) in GKO mice with massive granulocyte infiltration. Hematoxylin and eosin. Magnification, ×200.

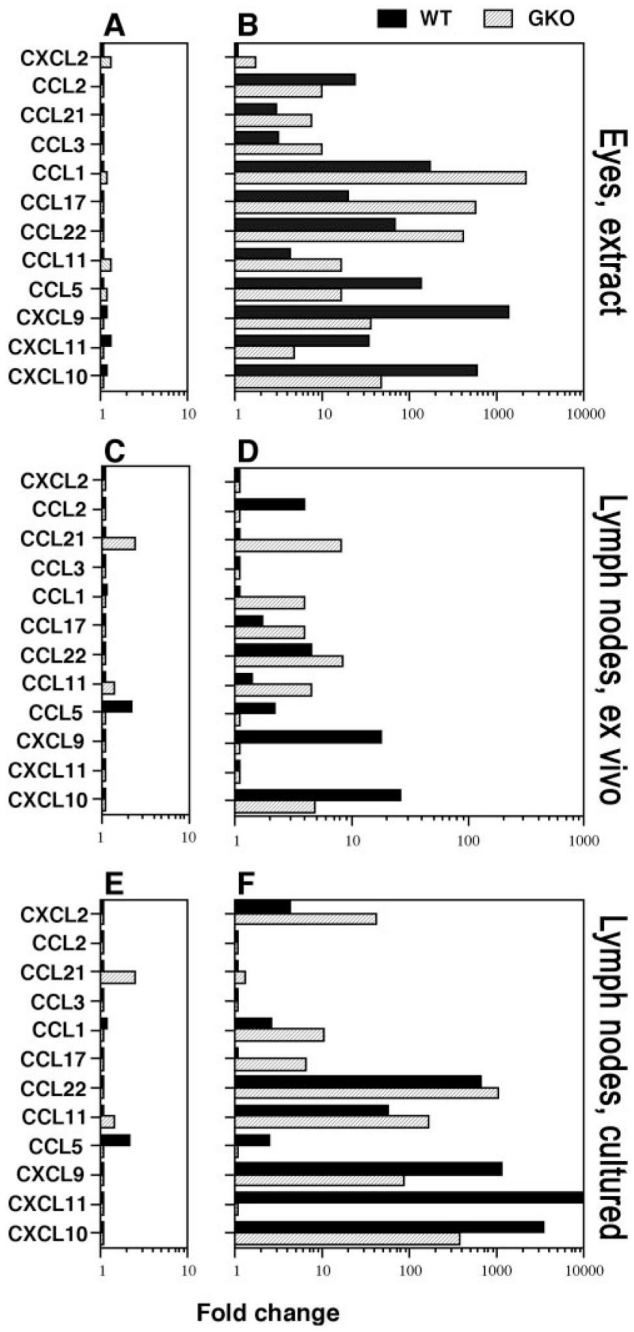

Figure 3.

Chemokine mRNA expression by real-time RT-PCR in eyes, lymph nodes, or lymph node cells stimulated with IRBP from WT and GKO mice. EAU was induced by immunization with IRBP/CFA and PT, and RNA extraction, real-time RT-PCR were performed. The relative changes in gene expression were calculated using the $2^{-\Delta\Delta CT}$ method. A twofold change was considered significant. (**A**) Chemokine expression in normal eyes versus (**B**) in eyes at EAU onset, 12 days after immunization. (**C**) Chemokine expression in normal lymph nodes versus (**D**) in lymph nodes from mice 3 days after IRBP immunization. (**E**) Background chemokine expression in draining lymph node cells 21 days after immunization cultured with medium

alone versus (**F**) in lymph nodes stimulated with IRBP overnight. The experiment was repeated twice with similar results. LN, lymph node.

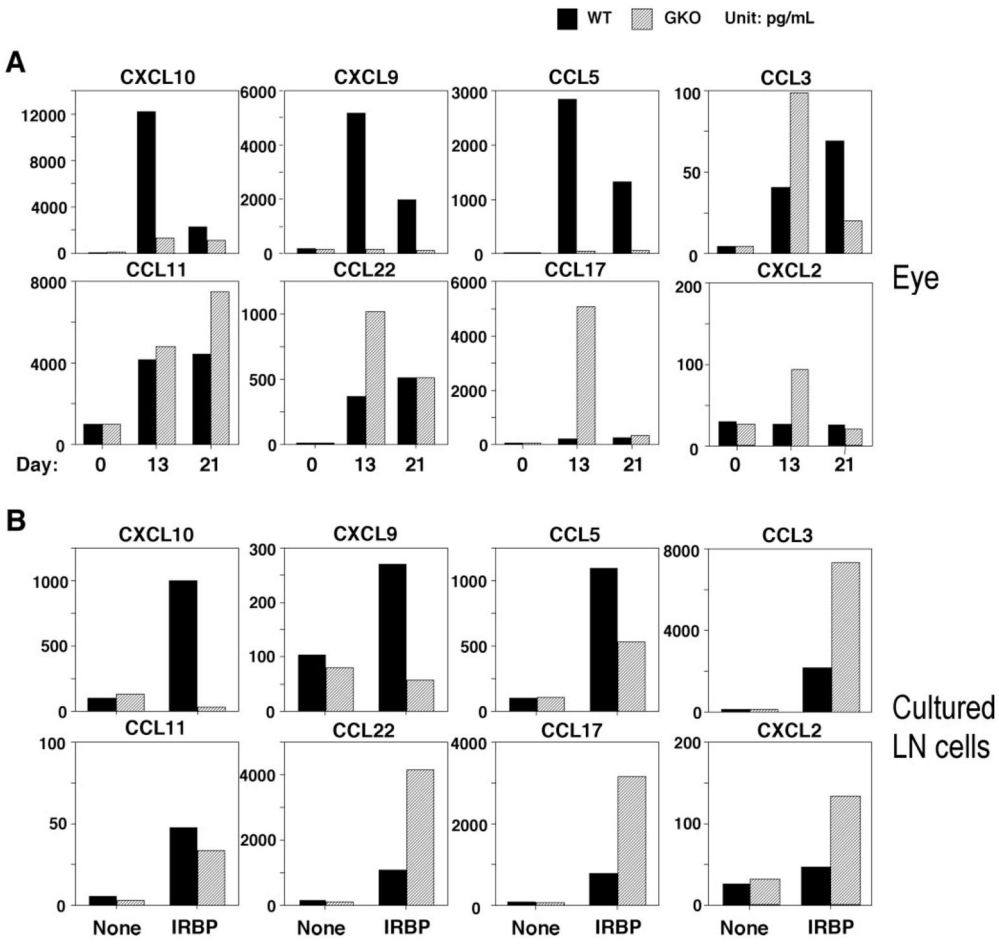

Figure 4.

Chemokine protein in eyes and in culture supernatant of draining lymph node cells from the mice immunized with IRBP. EAU was induced by immunization with IRBP/CFA and PT. (**A**) The eyes from day 0 (normal eyes), day 13 (1 day after disease onset), and day 21 (mature of the disease) after immunization were collected, and eye extract was prepared. (**B**) Lymph node cells harvested 21 days after immunization from IRBP-immunized mice were pooled within groups, and cultures of $5 \prime 10^6$ cells/mL were stimulated with IRBP. The supernatants were collected after 48 hours. Shown is chemokine content as assayed by ELISA in eye extracts and in culture (a representative experiment of three). Samples were pooled for analysis, therefore no error bars could be generated. LN, lymph node.

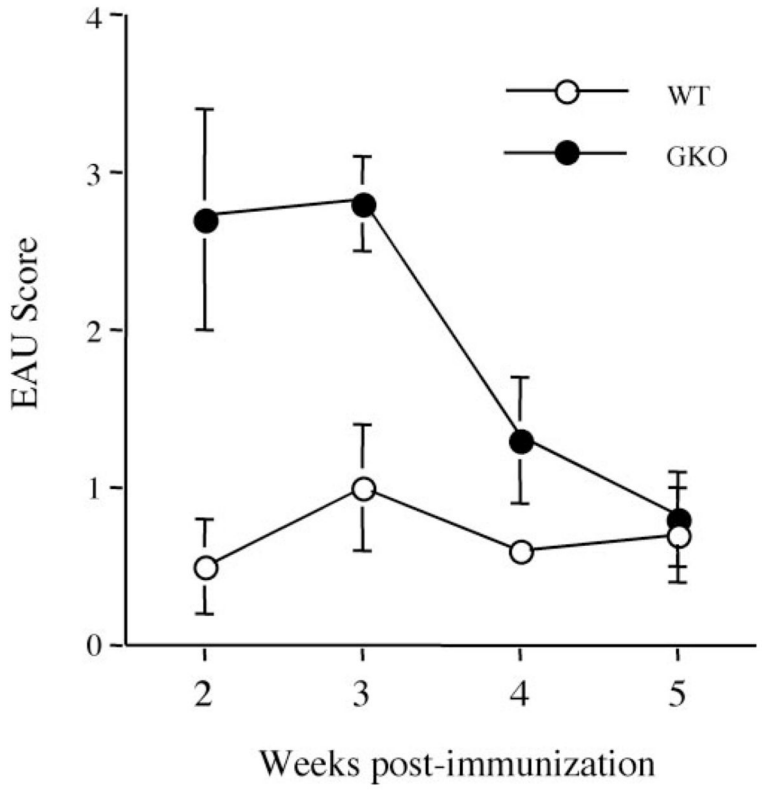

Figure 5.
Kinetics of disease progression in GKO and WT mice. GKO mice (n = 11) and control WT mice (n = 10) were immunized with 150 μg IRBP emulsified in CFA and received 0.5 μg of PT IP. Clinical development of disease was followed by fundus examination at the specified time points after immunization. The EAU score is the average of all the mice in the group ± SE.

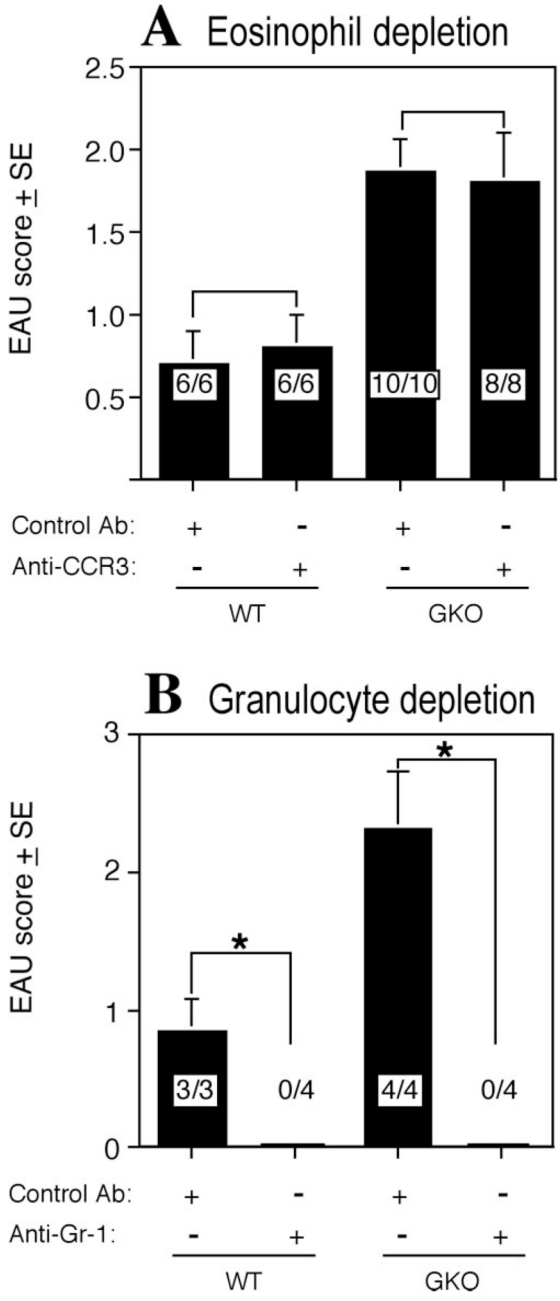

Figure 6.

Effect of eosinophil or granulocyte depletion on EAU development. EAU was induced by immunization with IRBP in CFA plus PT. (**A**) Mice were injected IP with 0.5 mg anti-CCR3 Ab daily from day −1 to day 13. Shown is a representative experiment of three. (**B**) Mice were injected IP with 0.1 mg of anti-Gr-1 Ab on days −1, 3, 6, 9, 12, and 15, Shown is a representative experiment of two. EAU scores were evaluated by histopathology 21 days after immunization. The score is the average of all the mice in the group. EAU incidence (positive/total) is shown within the bars. *Statistically significant difference in scores versus the untreated group ($P < 0.05$).

Table 1

CBCs in Anti-GR1-Depleted Anti-CCR3-Treated Mice

	Percentage (%)			Absolute (10007/μL)		
	Control Ab	**Anti-Gr1**	**Anti-CCR3**	**Control Ab**	**Anti-Gr1**	**Anti-CCR3**
Poly	9.75 ± 0.35	0.60 ± 0.50	7.90 ± 1.13	0.67 ± 0.02	0.02 ± 0.00	0.52 ± 0.05
Ly	83.60 ± 0.71	94.65 ± 0.07	88.45 ± 2.47	5.75 ± 0.01	4.08 ± 0.04	5.87 ± 0.45
Mo	5.05 ± 0.49	4.65 ± 0.21	3.50 ± 1.27	0.35 ± 0.04	0.31 ± 0.01	0.23 ± 0.07
Eo	1.30 ± 0.71	0.10 ± 0.08	0.10 ± 0.00	0.11 ± 0.03	0.01 ± 0.01	0.01 ± 0.00
Ba	0.30 ± 0.14	0.00 ± 0.00	0.15 ± 0.07	0.02 ± 0.01	0.00 ± 0.00	0.01 ± 0.00

Poly, polymorphonuclear leukocytes; Ly, lymphocytes; Mo, monocyte/macrophages; Eo, eosinophils; Ba, basophils.

Table 2

Gene Expression in EAU Onset Eyes, Draining Lymph Nodes, and IRBP-Stimulated T cells

	Eyes*			Lymph Nodes†			Cultured T Cells‡		
Gene	**WT**	**GKO**	**WT:GKO§**	**WT**	**GKO**	**WT:GKO§**	**WT**	**GKO**	**WT:GKO§**
Ccl1	2.17	3.38	−1.56	1.05	1.90	−1.80	1.54	2.57	−1.67
Ccl11	0.95	1.57	−1.65	1.17	2.05	−1.75	1.90	1.98	
Ccl12	1.48	1.63		0.93	0.98		1.17	0.99	
Ccl17	2.43	3.99	−1.64	1.30	1.86		1.45	7.99	−5.51
Ccl19	1.09	1.38		1.10	1.48		1.21	0.98	
Ccl2	1.91	1.77		1.61	1.02	1.58	1.24	1.01	
Ccl20	0.87	1.07		1.37	1.33		0.93	0.98	
Ccl21	1.67	2.41		1.09	2.45	−2.25	0.95	1.96	−2.06
Ccl22	1.68	2.72	−1.62	0.96	1.70	−1.77	1.59	2.93	−1.84
Ccl24	1.60	1.92		1.12	2.81	−2.51	2.17	0.97	2.24
Ccl25	0.84	1.27		0.89	1.13		1.34	0.98	
Ccl27	1.22	0.99		1.01	0.79		1.26	0.98	
Ccl28	1.33	1.70		0.96	1.37		1.22	1.00	
Ccl3	1.20	2.12	−1.76	1.45	1.42		1.24	1.52	
Ccl4	0.95	0.96		1.46	1.18		0.91	1.00	
Ccl5	3.61	1.16	3.11	2.92	1.21	2.41	3.03	0.93	3.26
Ccl6	1.35	1.10		1.03	1.22		1.32	0.97	
Ccl7	1.29	1.54		0.74	1.37		1.11	0.98	
Ccl8	1.30	1.10		0.93	1.24		1.61	0.97	1.66
Ccl9	1.14	1.02		1.23	0.77		1.66	0.99	1.68
Cx3cl1	1.28	1.16		1.32	0.91		1.30	1.01	
Cxcl1	0.96	1.13		1.00	0.88		1.10	0.96	
Cxcl10	4.12	2.60	1.58	3.82	1.71	2.23	6.04	1.96	3.08
Cxcl11	2.62	1.49	1.76	1.00	1.03		5.53	0.98	5.64
Cxcl12	0.90	1.23		1.03	0.91		1.51	1.27	
Cxcl13	1.14	0.87		1.72	1.58		1.42	0.98	
Cxcl14	1.31	0.96		1.50	1.37		1.10	0.98	
Cxcl15	1.21	1.75		0.82	1.43		1.51	1.00	1.51

Invest Ophthalmol Vis Sci. Author manuscript; available in PMC 2009 October 2.

Gene	Eyes*			Lymph Nodes†			Cultured T Cells‡		
	WT	GKO	WT:GKO§	WT	GKO	WT:GKO§	WT	GKO	WT:GKO§
Cxcl16	1.10	1.03		1.53	1.79		1.07	1.00	
Cxcl2	1.31	1.74		1.17	1.21		1.38	2.97	−2.15
Cxcl4	1.45	1.14		1.58	0.96	1.65	1.24	0.99	
Cxcl5	0.87	1.13		1.45	1.35		1.19	1.02	
Cxcl7	1.30	1.18		0.93	1.34		1.46	1.00	
Cxcl9	3.75	1.57	2.39	2.75	1.17	2.35	4.95	1.99	2.49
Xcl1	1.28	1.13		0.99	0.95		1.54	1.05	

*m RNA levels are expressed as ratio of inflamed eyes to normal eyes (i.e. increase over baseline).

†mRNA levels in naïve lymph nodes are baseline for draining lymph nodes 3 days after immunization.

‡The baseline for IRBP-stimulated T cells is the mRNA level in the cells cultured with medium alone.

§Difference in expression between WT and GKO is shown as the ratio of increase in WT mice to the increase in GKO mice. Each value represents the relative increase in expression for a given chemokine in WT versus GKO mice. Minus values indicate that the expression in GKO mice is higher than in WT mice.

Table 3

Primer Sequences of Chemokines and GAPDH for Real-Time RT-PCR Using the Light Cycler

Chemokine Gene	Primer Sequence (5′–3′)	Fragment Size (bp)
CCL1	F: CGTGTGGATACAGGATGTTGACAG	125
	R: AGGAGGAGCCCATCTTTCTGTAAC	
CCL3	F: TGAATGCCTGAGAGTCTTGG	133
	R: TTGGCAGCAAACAGCTTATC	
CCL2	F: TAGGCTGGAGATCTACAAGAGG	277
	R: AGTGCTTGAGGTGGTTGTGG	
CCL5	F:CACCACTCCCTGCTGCTT-3	131
	R: ACACTTGGCGGTTCCTTC-3	
CCL11	F: GGCTGACCTCAAACTCACAGAAA	69
	R: ACATTCTGGCTTGGCATGGT	
CCL17	F: CAAGCTCATCTGTGCAGACC	219
	R: CGCCTGTAGTGCATAAGAGTCC	
CCL21	F: CAACCATTACATCTGCACGG	201
	R: TCATAGGTGCAAGGACAAGG	
CCL22	F: AAGACAGTATCTGCTGCCAGG	141
	R: GATCGGCACAGATATCTCGG	
CXCL2	F: CGCCCAGACAGAAGTCATAG	132
	R: TCCTCCTTTCCAGGTCAGTTA-3	
CXCL9	F: TTTTGGGCATCATCTTCCTGG	122
	R: GAGGTCTTTGAGGGATTTGTAGTGG	
CXCL10	F: CTTCTGAAAGGTGACCAGCC	187
	R: GTCGCACCTCCACATAGCTT	
CXCL11	F: AACAGGAAGGTCACAGCCATAGC	174
	R:TTTGTCGCAGCCGTTACTCG	
GAPDH	F: CTCATGACCACAGTCCATGC	201
	R: CACATTGGGGGTAGGAACAC	

F, forward; R, reverse.

Table 4

Changes in Composition of Infiltrating Cells in WT and GKO Mice

	Week 2		Week 3		Week 4		Week 5	
	WT (*n* = 8)	**GKO (*n* = 8)**	**WT (*n* = 24)**	**GKO (*n* = 23)**	**WT (*n* = 5)**	**GKO (*n* = 5)**	**WT (*n* = 6)**	**GKO (*n* = 6)**
Mo	44.5 ± 5.0	22.7 ± 4.5	38.0 ± 9.9	21.0 ± 5.8	38.0 ± 7.1	35.5 ± 5.2	40.0 ± 1.4	54.0 ± 11.1
Ly	35.0 ± 1.4	12.7 ± 3.1	41.5 ± 7.8	19.3 ± 5.7	50.5 ± 10.6	35.0 ± 6.5	46.5 ± 3.5	33.0 ± 8.2
Neut	19.0 ± 2.8	54.0 ± 4.0	13.0 ± 7.1	47.7 ± 7.5	10.0 ± 2.8	24.0 ± 5.1	9.5 ± 0.7	10.0 ± 1.4
Eo	2.5 ± 0.7	10.7 ± 3.6	2.0 ± 0.6	13.0 ± 3.8	3.0 ± 1.9	5.6 ± 2.6	2.0 ± 1.2	3.0 ± 2.2

Composition of infiltrating cells in uveitic eyes as a function of time after immunization is expressed as a percentage of each cell type out of total. Mo, mononcyte/macrophages; Ly, lymphocytes; Neut, neutrophils; Eo, eosinophils.